# Energy Component Analysis of $\pi$ Interactions

C. DAVID SHERRILL*

*Center for Computational Molecular Science and Technology, School of
Chemistry and Biochemistry, and School of Computational Science and
Engineering, Georgia Institute of Technology, Atlanta, Georgia 30332,
United States*

## CONSPECTUS

Fundamental features of biomolecules, such as their structure, solvation, and crystal packing and even the docking of drugs, rely on noncovalent interactions. Theory can help elucidate the nature of these interactions, and energy component analysis reveals the contributions from the various intermolecular forces: electrostatics, London dispersion terms, induction (polarization), and short-range exchange−repulsion. Symmetry-adapted perturbation theory (SAPT) provides one method for this type of analysis.


Favorable Induction/Polarization
Electrostatic repulsion

In this Account, we show several examples of how SAPT provides insight into the nature of noncovalent $\pi$-interactions. In cation−$\pi$ interactions, the cation strongly polarizes electrons in $\pi$-orbitals, leading to substantially attractive induction terms. This polarization is so important that a cation and a benzene attract each other when placed in the same plane, even though a consideration of the electrostatic interactions alone would suggest otherwise. SAPT analysis can also support an understanding of substituent effects in $\pi$−$\pi$ interactions. Trends in face-to-face sandwich benzene dimers cannot be understood solely in terms of electrostatic effects, especially for multiply substituted dimers, but SAPT analysis demonstrates the importance of London dispersion forces. Moreover, detailed SAPT studies also reveal the critical importance of *charge penetration effects* in $\pi$-stacking interactions. These effects arise in cases with substantial orbital overlap, such as in $\pi$-stacking in DNA or in crystal structures of $\pi$-conjugated materials. These charge penetration effects lead to attractive electrostatic terms where a simpler analysis based on atom-centered charges, electrostatic potential plots, or even distributed multipole analysis would incorrectly predict repulsive electrostatics. SAPT analysis of sandwich benzene, benzene−pyridine, and pyridine dimers indicates that dipole/induced-dipole terms present in benzene−pyridine but not in benzene dimer are relatively unimportant. In general, a nitrogen heteroatom contracts the electron density, reducing the magnitude of both the London dispersion and the exchange−repulsion terms, but with an overall net increase in attraction.

Finally, using recent advances in SAPT algorithms, researchers can now perform SAPT computations on systems with 200 atoms or more. We discuss a recent study of the intercalation complex of proflavine with a trinucleotide duplex of DNA. Here, London dispersion forces are the strongest contributors to binding, as is typical for $\pi$−$\pi$ interactions. However, the electrostatic terms are larger than usual on a fractional basis, which likely results from the positive charge on the intercalator and its location between two electron-rich base pairs. These cation−$\pi$ interactions also increase the induction term beyond those of typical noncovalent $\pi$-interactions.
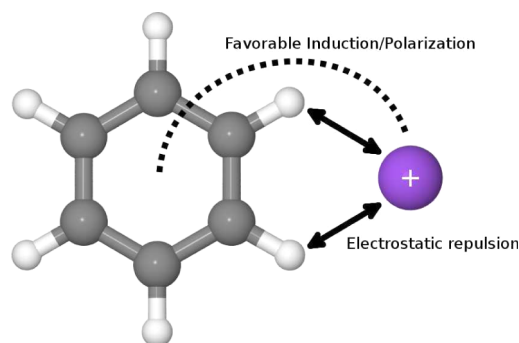
## Introduction

Noncovalent interactions are ubiquitous in chemistry, biology, and materials science. They control diverse phenomena including boiling points of liquids, solvation energies, and the structures of molecular crystals. $\pi$-Interactions constitute one of the most important chemical classes of noncovalent interactions, spanning various subtypes ($\pi$−$\pi$, cation−$\pi$, C−H/$\pi$, etc.)[1,2] and contributing to biomolecular structure, drug binding, and the structure and properties of $\pi$-conjugated materials of interest in organic electronics and photonics.

There are a number of important questions regarding various classes of noncovalent interactions, such as how strong they are, how they change with changing geometry,

and how they are affected by the introduction of a substituent or heteroatom. A number of clever chemical model systems have been designed to address these questions (for a recent review, see ref 3). For example, the "molecular torsion balance" of Wilcox and co-workers features a "closed" conformer with a T-shaped $\pi-\pi$ interaction and an "open" conformer without this interaction.[4,5] The equilibrium constant between these two conformers can be obtained by NMR, and it can be tabulated as a function of various substituents on one of the $\pi$ systems. Unfortunately, these data can be difficult to interpret, because the equilibrium constant is also influenced by differences in the solvent-accessible area of the closed and open forms,[6,7] and in principle, substituents may influence solvent–solute interactions more strongly in one of the conformers than the other. Such complicating considerations can be avoided by performing gas-phase studies on small van der Waals dimers, but these experiments can be difficult and often require mass selection techniques to obtain the dimer of interest instead of a larger cluster. Moreover, the experiments often also have to employ supersonic jet expansions to achieve low temperatures and thereby isolate one or a handful of the most energetically favorable geometric configurations. Even so, the potential energies of van der Waals dimers tend to be very flat, meaning that even at low temperatures, the systems can be fluxional without a well-defined geometric structure.[8]

Theory offers some assistance, because it is easy in an electronic structure computation to exactly fix the geometry of some noncovalent contact and to compute the interaction energy apart from secondary interactions or solvent effects. This allows one to directly probe the strength of intermolecular interactions, and how they vary with substituents and heteroatoms. Scanning over various geometries leads to information about geometric dependence. Unfortunately, such theoretical studies are not without their challenges. In particular, rather sophisticated (and computationally costly) electronic structure methods are required to obtain "definitive" results for noncovalent interactions. At present, the favored benchmark-quality approach is coupled-cluster theory through perturbative triple excitations [CCSD(T)] with large basis sets, or more practically, second-order perturbation theory (MP2) complete-basis-set extrapolations plus a coupled-cluster correction evaluated in a smaller basis set.[9] Various approximate electronic structure methods do reasonably well, or very poorly indeed (depending on the method), compared with the benchmark results.

Although accurate theoretical binding energies for noncovalent interactions can be enormously helpful, they are often not enough, because even the theoretical data can remain hard to interpret. We have found that noncovalent interactions are significantly easier to understand with the aid of energy component analysis, which dissects the attraction between two monomers into various fundamental physical components, such as electrostatics (e.g., charge–charge, charge–dipole, dipole–dipole, etc.), London dispersion forces (e.g., instantaneous dipole/induced dipole), induction/polarization forces (e.g., dipole/induced-dipole), and exchange–repulsion terms. In this Account, we will provide a few examples of how an energy component analysis has been helpful in providing deeper insight into the physics of noncovalent $\pi$-interactions.

## Symmetry-Adapted Perturbation Theory

Among energy component analysis methods, we find symmetry-adapted perturbation theory (SAPT)[10,11] to be arguably the most physically well-motivated. In this approach, one uses intermolecular perturbation theory to compute the strength of the intermolecular interaction. Each term in the interaction (electrostatics, dispersion, induction, and exchange–repulsion) falls out of the theory in a very clear and natural way. By contrast, some other approaches to energy component analysis make seemingly arbitrary choices about how to partition the various energy components. On the other hand, as a perturbation theory, SAPT can break down if the perturbation gets too large (i.e., if the interacting fragments get too close).[12] However, in practice, we have not found this to be a serious issue in any of the systems we have studied to date, and there are some remedies in cases where this starts to become an issue.[12,13]

The simplest and most basic SAPT approach is designated SAPT0, and this implies that one does a Hartree–Fock molecular orbital computation on each monomer and then treats the intermolecular interaction with second-order perturbation theory. The theory has been formulated to higher orders to include intramolecular electron correlation effects (e.g., SAPT2 includes these terms through second-order). The most complete levels of SAPT provide interaction energies very close to benchmark CCSD(T) values (but with similar computational costs). Fortunately, we have found that low-order SAPT0, when judiciously paired with the right basis sets (of polarized double-$\zeta$ quality), provides reasonably good interaction energies that are sufficient for obtaining correct trends and for understanding the qualitative physics of noncovalent interactions in most cases.[14] As an alternative to wave function-based SAPT, there is also a variant based on density functional theory,[15,16] named DFT-SAPT or SAPT(DFT). This approach provides a more computationally

efficient way to handle intramolecular correlation and provides very accurate interaction energies.[17]

## Cation−$\pi$ Interactions

Cation−$\pi$ interactions represent one of the clearest examples of the usefulness of energy component analysis for noncovalent interactions. These interactions are important to a number of biochemical processes, including acetylcholine binding, biosynthesis of steroids, and ion selectivity in $K^+$ channels.[18] In the gas phase, the interaction energy between $K^+$ and a benzene can be as strong as −19 kcal mol$^{-1}$ (noncovalent interaction energies are usually reported as negative numbers, with more negative values representing stronger interactions); this interaction is even stronger than the interaction between $K^+$ and a $H_2O$ molecule.[19] The strength of this cation−$\pi$ interaction can be rationalized on the basis of a strong electrostatic interaction between the positively charged cation and the negatively charged $\pi$-cloud.

Based on this simple picture, however, it is hard to understand why gas-phase computations also demonstrate an attraction between a $Na^+$ cation and a benzene when the cation and the benzene are in the same plane.[21] Nevertheless, as shown in Figure 1, the total SAPT interaction energy for the in-plane configuration is also negative (attractive) around the minimum of the potential curve. This result is counterintuitive because the closest atoms to the cation are aromatic hydrogen atoms, which have a partial positive charge. The SAPT energy component analysis explains why this interaction is attractive. As one can see from the energy components plotted in the bottom panel of Figure 1, the electrostatic interaction is indeed unfavorable, as one would guess. However, there is a strongly attractive induction (polarization) term that leads to overall favorable interactions in the side-on geometry. Given that one of the monomers is a cation and the other has polarizable electrons, in retrospect it is not too surprising that there could be a strong induction component (and indeed an earlier study of the on-top geometry using energy component analysis highlighted the importance of induction).[22] Studies including the implicit solvent polarized continuum model (PCM) indicate that these side-on cation−benzene interactions remain favorable even in water for $Li^+$, and they remain favorable for a number of additional cations ($Na^+$, $K^+$, $NH_4^+$) at near-side-on geometries.[21]

## $\pi$−$\pi$ Interactions and Their Substituent Effects

$\pi$−$\pi$ Interactions influence protein folding and many drug binding complexes,[1,23] and they are critical for stabilizing the structure of DNA and RNA.[24] Understanding how $\pi$−$\pi$
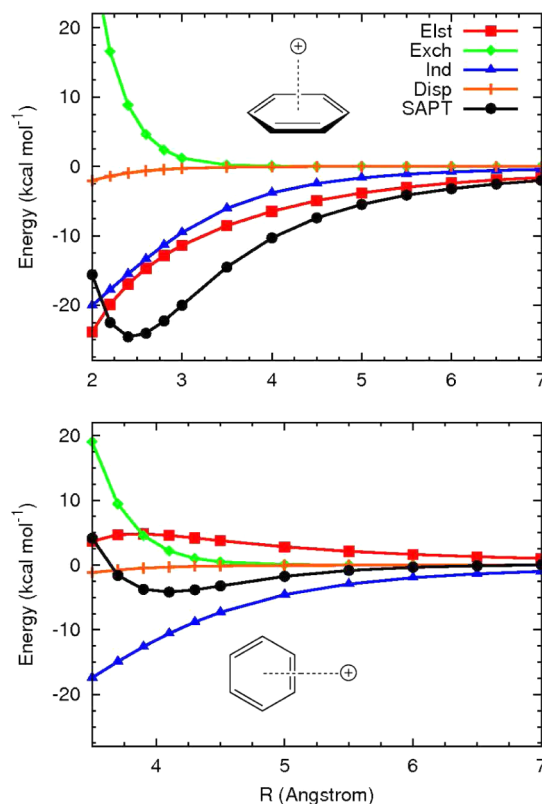


**FIGURE 1.** Energy components (electrostatics, exchange−repulsion, induction, and London dispersion terms) as a function of cation−benzene separation for an on-top configuration (top panel) and for an in-plane configuration (bottom panel); the total interaction energy is given by the black curves. Results using the SAPT0/jun-cc-pVDZ level of theory (adapted from ref 20).

interactions can be modified by substituents or heteroatoms is of fundamental importance for advances in drug design, exploration of non-natural nucleic acid analogs, and crystal engineering of organic materials.

$\pi$−$\pi$ Interactions often occur in parallel geometries (e.g., stacking of nucleobases in DNA). Typically, the aromatic rings are not strictly cofacial ("sandwich" configuration), but are offset ("parallel-displaced" configuration, see Figure 2). Nevertheless, near-sandwich configurations are observed in some synthesized model systems,[25−28] and the sandwich structures have remained popular in theoretical studies because they are simpler geometrically. Another common interaction motif is the perpendicular, edge-to-face ("T-shaped") configuration. Both parallel-type and perpendicular-type configurations (and intermediate configurations) are frequently observed in biological systems and in organic materials. Benchmark-quality electronic structure computations using a combination of small-basis CCSD(T) and large-basis MP2 energies were critical in resolving controversies about the relative energetics of these prototype configurations.[29,30]
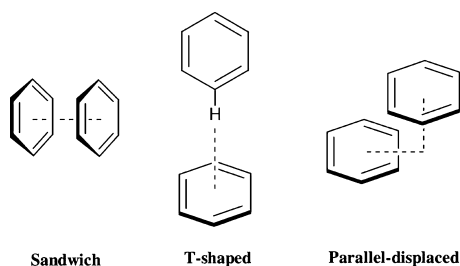
**FIGURE 2.** Prototypical $\pi-\pi$ geometric configurations of the benzene dimer.
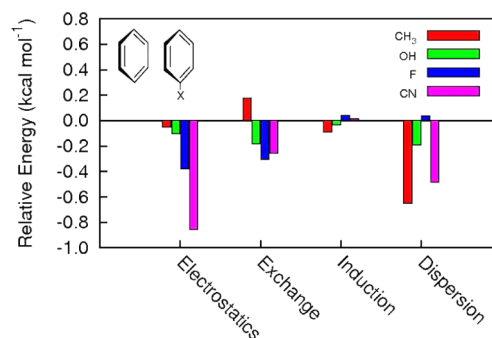


**FIGURE 3.** Interaction energy components relative to benzene dimer for monosubstituted sandwich benzene dimers at a fixed intermolecular distance of 3.7 Å (SAPT2/jun-cc-pVDZ level of theory, ref 34).

Substituent effects in $\pi-\pi$ interactions are most commonly understood through the Hunter–Sanders rules,[31] which state that the primary effect of substituents is a change in the electrostatic interaction as the substituent donates or withdraws electron density from the electron-rich (and thus negatively charged) $\pi$ cloud. These rules resulted from an analysis that attempted to reconcile available experimental data at the time with a very simple model of electrostatics: for each atom contributing one electron to an aromatic $\pi$-system (e.g., an aromatic carbon in benzene), the model placed a $+1$ charge at each nucleus (representing the $\sigma$-framework) and two $-1/2$ charges displaced above and below the plane of the aromatic (representing the $\pi$-cloud). According to the Hunter–Sanders rules, in an idealized face-to-face sandwich configuration, one would expect electron-withdrawing substituents to reduce unfavorable electrostatic interactions between the negatively charged $\pi$-clouds, and of course electron-donating substituents should have the opposite effect. Theoretical studies of gas-phase monosubstituted benzene dimers, however, indicated that *both* electron-donating and electron-withdrawing substituents increase the attraction between two benzenes in the sandwich orientation.[32,33]

SAPT analysis provides very helpful insight into how this unexpected situation can occur. Figure 3 shows changes in the interaction energy components due to substituents in various monosubstituted sandwich benzene dimers. The electron-withdrawing CN and F substituents cause a much more favorable electrostatic term than in the benzene dimer, which is consistent with the Hunter–Sanders view. However, for a weakly electron-donating $CH_3$ substituent, the major change in interaction energy is not a more repulsive electrostatic term, but instead a more attractive London dispersion term. Differential dispersion effects are neglected in the Hunter–Sanders view, but they are critical to understanding the increased gas-phase binding of the toluene–benzene sandwich.

A subsequent computational study by Wheeler and Houk[35] on a larger number of monosubstituted benzene dimers argued that, although all substituents increase the

strength of sandwich $\pi-\pi$ interactions, the *general trend* remains determined by electrostatic effects. The authors found a good correlation between the energy stabilization due to the substituent and its Hammett parameter $\sigma_m$ (which is supposed to represent the electron donating/withdrawing character of the substituent). Wheeler and Houk also made the important and totally unexpected discovery that substituent effects are basically the same in $HX \cdots C_6H_6$ model systems as they are in $C_6H_5X \cdots C_6H_6$ sandwiches. This implies that the substituents are *not* changing the $\pi$-cloud density/charge as supposed by Hunter and Sanders[31] but instead they are contributing through direct interactions between the substituent and the other aromatic system (this is consistent with previous experimental[36,37] and theoretical[38] work suggesting the importance of direct substituent–$\pi$ interactions). This general picture has been supported by subsequent theoretical work,[39–42] and in fact, it has been extended to a "local interaction" model in which Wheeler has shown that the substituent interacts primarily with just the nearest vertex of the other ring.[42]

Despite Wheeler and Houk's finding of a good correlation between a substituent's effect on the binding energy and the electrostatic character of the substituent (as given by the $\sigma_m$ parameter), we nevertheless felt that the importance of differential London dispersion effects should be emphasized. After all, if dispersion is important enough that all substituted sandwich dimers are stabilized relative to the parent benzene dimer (despite the presumably unfavorable electrostatic terms for the electron-donating substituents), then there should be situations where this small stabilizing effect could become a large one. On the basis of the general additivity of substituent effects in multiply substituted sandwich dimers found in one of our previous theoretical studies,[38] we expected that dispersion contributions could become quite large for multiply substituted dimers. Hence, in
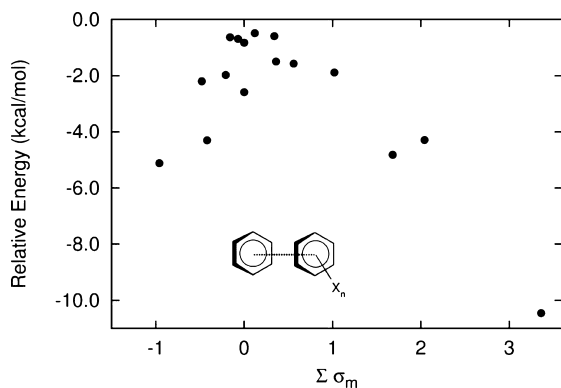
**FIGURE 4.** Breakdown of the correlation between relative binding energies and $\Sigma\sigma_m$ for multiply substituted sandwich benzene dimers (results at the MP2/aug-cc-pVDZ level of theory, adopted from ref 43).



**FIGURE 5.** SAPT electrostatic, dispersion, and total interaction energies of substituted sandwich benzene dimers relative to the unsubstituted benzene dimer at their respective equilibrium geometries (SAPT0/jun-cc-pVDZ level of theory). Relative electrostatic energies from a (less reliable) distributed multipole analysis (DMA) are also plotted. Adapted from ref 50.

2009 we computed the binding energy of several mono-substituted, 1,3,5-trisubstituted, and hexa-substituted benzene dimers.[43] As anticipated, we found a breakdown (see Figure 4) of the correlation between the relative interaction energies and the substituent's electrostatic character (as measured by $\Sigma\sigma_m$), presumably because the systems with multiple electron-donating substituents had multiple additional stabilizing London dispersion contacts.

Given the strong theoretical evidence for the importance of differential dispersion contributions to substituent effects in $\pi$-stacking interactions, it is perhaps somewhat surprising that only limited experimental evidence[27,44] appears to directly or indirectly support the theoretical results. A likely explanation for the discrepancy is that the computations are typically carried out in the gas phase, whereas most experimental studies of substituent effects have been in solution. Solvent may damp out some of the dispersion contribution to substituent effects,[37] and Hunter and co-workers have proposed models that appear to work well for torsion balances and zipper complexes by considering only $\pi-\pi$ vs solvent$-\pi$ electrostatic interactions[45,46] (although these models appear to be formulated for edge-to-face interactions, where differential dispersion effects appear to be somewhat less important[34,38,47]). More work on the influence of solvent on substituent effects is warranted.

As our new SAPT program[14,48] was becoming available in 2010, we began a follow-up study to verify some of our assumptions about the underlying causes of the substituent effects. While our work was underway, a similar study was published by Lewis and co-workers.[49] One surprising result of Lewis's work was that the *electrostatic* contribution to binding in *all* substituted dimers was more favorable than in the parent benzene dimer. We had assumed that stronger bin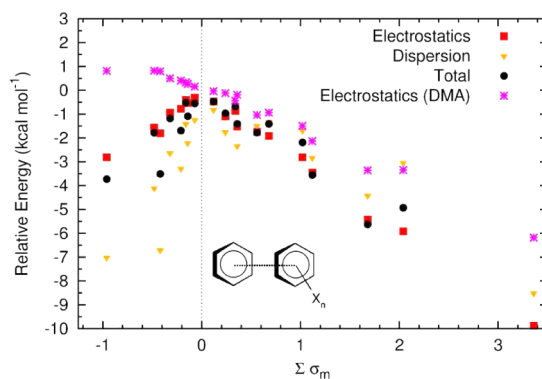ding for electron-donating substituents was solely due to more favorable London dispersion forces, which apparently overcame any unfavorable electrostatic contribution. That the electrostatic contribution itself was also more favorable seemed to contradict any common-sense picture of this problem. This issue was left unexplained in the work by Lewis, but it was confirmed by our own SAPT results. After some further study, we saw that SAPT analysis was once again the key to obtaining a deeper understanding of $\pi$-interactions.[50]

Figure 5 illustrates the problem, plotting energies relative to benzene dimer vs the sum of the Hammett $\sigma_m$ parameters for the substituents. As expected, the dispersion contribution to the relative energies is very large for the multiply substituted dimers, whether or not the substituents are electron-donating or electron-withdrawing, with magnitude increasing with the number of substituents. However, the surprising feature is the inverted V-shaped graph of the relative electrostatic energies. A key to understanding this phenomenon is to replot the relative electrostatic energies as a function of the distance between the two monomers; if we do this (see Figure 6), we see that the correlation with $\Sigma\sigma_m$ is restored at large distances and only breaks down at shorter distances of around 4.0 Å or less. Note that the equilibrium distances for these systems (3.45–3.95 Å) and for parallel $\pi-\pi$ interactions in general are below this cutoff. For example, the interplanar distance between base pairs in DNA is only about 3.4 Å.

Given this information, the behavior of these systems becomes clear. At long distances, our intuition that electron-donating and electron-withdrawing substituents should have opposite electrostatic contributions is correct. However, at short distances, an additional contribution enters into the physics: charge penetration. As two electron clouds overlap, there is a favorable electrostatic contribution coming from the
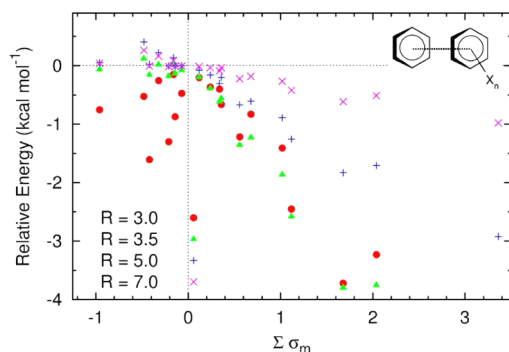
**FIGURE 6.** SAPT electrostatic energies for multiply substituted sandwich benzene dimers relative to the unsubstituted benzene dimer at various fixed intermolecular distances (SAPT0/jun-cc-pVDZ level of theory). Adapted from ref 50.



**FIGURE 7.** Sandwich configurations of the benzene, benzene–pyridine, and pyridine dimers.

fact that diffuse electron clouds do not repel each other as much as point charges do, so that the electron–nuclear attraction terms become slightly larger in magnitude than the sum of the nuclear–nuclear and electron–electron repulsion terms. This charge penetration term grows very rapidly as the distance between the monomers decreases (of course, the exchange–repulsion term also grows very rapidly and overwhelms any attraction from charge penetration at sufficiently short distances). Because any substituent will have more electron density than a hydrogen atom, any substituent leads to more favorable charge penetration terms than H atom, regardless of the electron-donating or electron-withdrawing nature of the substituent. To further test our hypothesis that charge penetration is responsible for the behavior of the electrostatic term, we also computed electrostatics using a distributed multipole analysis (DMA) including up to quadrupole–quadrupole terms. The DMA results fit our earlier intuition about the electrostatic term and provide a correlation between electrostatics and $\Sigma\sigma_m$, but they do not fit the more complete and more rigorous quantum-mechanical SAPT electrostatic energies. The DMA model should be rather complete except for its failure to account for charge penetration terms. Hence, the unusual behavior of the SAPT electrostatic contributions appears to be due to charge penetration terms.

In this section, we have focused on idealized sandwich geometries because they are simpler to study than other geometries (all hydrogens in the parent system are symmetry-equivalent, so there are fewer distinct ways to arrange the substituents). In addition, the substituent effects in the sandwich configuration are the most counterintuitive and thus the most interesting. Nevertheless, substituent effects have also been studied computationally in T-shaped and parallel-displaced geometries,[34,39,47,51–53] usually employing energy component analysis.
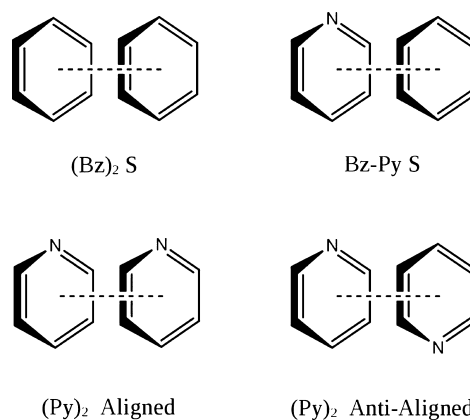
## Heteroatom Effects in π–π Interactions

It is also interesting to address how heteroatoms affect π–π interactions, especially given the heteroatoms present in the nucleobases of DNA. To probe this question directly, we studied a simple model system (pyridine dimer) in many geometries, and we compared results to those from the benzene dimer and from the pyridine–benzene dimer[54] (related studies have been carried out on other systems).[55,56] Again, energy component analysis with SAPT was very helpful in understanding the heteroatom effects. For present purposes, let us consider just sandwich geometries, and for the pyridine dimer, let us consider the limiting cases where the dipoles are aligned or antialigned (see Figure 7). Table 1 presents the SAPT2 analysis of the different energy components.

First, we note that the antialigned pyridine dimer is the most stabilized dimer ($-3.05$ kcal mol$^{-1}$), and the aligned pyridine dimer is the least stabilized ($-1.69$ kcal mol$^{-1}$). This might have been expected based on consideration of dipole–dipole interactions, and indeed, the electrostatic interactions are strongly favorable ($-1.29$ kcal mol$^{-1}$) for the antialigned configuration and only very weakly favorable ($-0.05$ kcal mol$^{-1}$) for the aligned dimer. However, arguments based on dipole–dipole interactions may be oversimplified for this system, where the π-clouds are in close contact (3.8 Å) and the multipole picture may no longer be valid. First, the electrostatic term is attractive for all four model sandwich complexes, even for the aligned pyridine dimer. We attribute this to favorable charge penetration.[33] Second, the benzene–pyridine sandwich exhibits an electrostatic attraction ($-0.80$ kcal mol$^{-1}$) that is more than half of the separation between the aligned and the antialigned pyridine dimers. The trends in the electrostatic contributions may

**TABLE 1.** Energy Component Analysis (in kcal mol$^{-1}$) of Sandwich Configurations of the Benzene, Benzene–Pyridine, and Pyridine Dimers[a]

|  | elst | ind | exch | disp | net disp[b] | SAPT2[c] |
|---|---|---|---|---|---|---|
| (Bz)$_2$ | −0.48 | −0.28 | 4.52 | −5.68 | −1.17 | −1.92 |
| Bz−Py | −0.80 | −0.26 | 4.00 | −5.34 | −1.34 | −2.39 |
| (Py)$_2$ aligned | −0.05 | −0.21 | 3.57 | −5.00 | −1.44 | −1.69 |
| (Py)$_2$ antialigned | −1.29 | −0.25 | 3.49 | −5.00 | −1.51 | −3.05 |

[a]Energies at an intermolecular separation of 3.8 Å (SAPT2/jun-cc-pVDZ level of theory, from ref 54). [b]Net dispersion is the sum of the exchange and dispersion components. [c]Total SAPT2 interaction energy.

be governed more by direct interactions between the electron-rich nitrogen atom on pyridine and an electron-deficient aromatic hydrogen of the opposing ring than they are by dipole–dipole interactions.

Next, we note that the dispersion term is most favorable for the benzene dimer and least favorable for the pyridine dimers, with the pyridine–benzene value falling in between. This is consistent with the smaller polarizability of pyridine compared with benzene. The exchange–repulsion term has the opposite trend, being most repulsive for benzene dimer and least repulsive for pyridine dimer. This seems consistent with the more electronegative heteroatom reducing the spatial extent of the electron density in pyridine compared with benzene, reducing the amount of orbital overlap and hence exchange–repulsion. Because the trends in dispersion and exchange–repulsion are opposite and roughly equal in magnitude for many π-stacked systems, it is particularly interesting to examine the sum of these two terms (which we have called "net dispersion" in π-stacked systems). Here, we see that the heteroatom reduces exchange–repulsion more than it decreases dispersion, so that overall the more substituted systems have more favorable "net dispersion" terms. This is an example of the utility of a quantitative SAPT analysis; although conceivably one might have correctly guessed ahead of time the trends in the electrostatic, dispersion, and exchange terms, it would be difficult indeed to guess whether the changes in dispersion would have been more or less than those in exchange.

Finally, we notice that the induction term is nearly constant for all four of these systems, around −0.25 kcal mol$^{-1}$. This is perhaps surprising, given that pyridine dimer or pyridine–benzene both should have dipole/induced-dipole contributions (included in the induction term), whereas benzene dimer should not. Indeed, one might have expected for this to be a significant difference between benzene dimer and the other dimers. However, SAPT clarifies that such terms are of little consequence for these systems. More generally, we have found induction (polarization) terms to be relatively unimportant in most of our SAPT
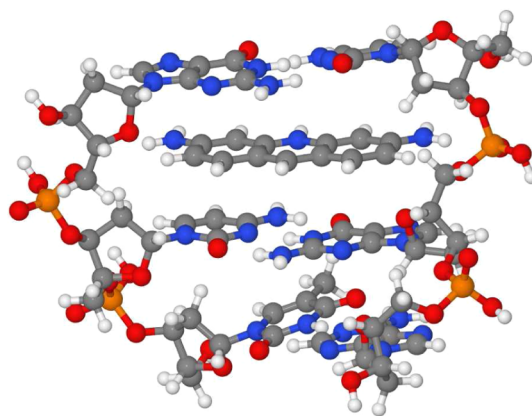


**FIGURE 8.** Intercalation complex of proflavine with a CGA segment of DNA, as studied in ref 48. Geometry taken from X-ray crystal structure (see ref 57). To simplify the computational procedure, some oxygens have been capped by hydrogens in lieu of placing sodium counterions.

studies to date, except for systems involving non-neutral monomers.

## DNA Intercalation

As a recent application[48] of our very efficient SAPT0 implementation,[14,48] we examined the intercalation of proflavine into a trinucleotide duplex of DNA (see Figure 8), based on an available X-ray crystal structure.[57] At 220 atoms and 2845 basis functions, this represents the largest SAPT0 computation reported to date. With three fused aromatic rings and a positive charge, proflavine is typical of DNA intercalators, which include some anticancer agents. That proflavine binds well to DNA is not surprising given the strong π-stacking resulting from an intercalation geometry. However, SAPT analysis allows us to quantify the binding and its origins in terms of the various fundamental intermolecular forces. London dispersion forces are by far the strongest attractive component in the binding (−67.6 kcal mol$^{-1}$). This suggests that in the design of strongly binding intercalators, the polarizability of the intercalator, not just its electrostatic properties, should be considered. The dominance of dispersion is consistent with results for many other π-stacked systems, like the sandwich benzene or pyridine dimers;[54] in the sandwich pyridine dimer, even when the dipoles are antiparallel, the electrostatic interaction is only a quarter of the dispersion interaction. Here, the electrostatic stabilization (−37.9 kcal mol$^{-1}$) is nearly half as large as the dispersion term, perhaps aided by the interaction of the electron-deficient cationic proflavine with the electron-rich nucleobases (as well as by contributions from charge-penetration terms, see above). Induction, at −11.4 kcal mol$^{-1}$, provides the remaining stabilization.

By comparing to a model system in which the backbone was removed, we determined that $\pi$-stacking only accounts for about 2/3 of the gas-phase binding energy, while two long hydrogen bonds between the intercalator and the backbone account for most of the remaining 1/3. This suggests that intercalation is not entirely a $\pi$-stacking phenomenon and that backbone interactions should be considered also.

## Conclusions

As illustrated by the above examples, energy component analysis via symmetry-adapted perturbation theory is very useful in understanding noncovalent $\pi$ interactions and their substituent and heteroatom effects. In particular, SAPT analysis has demonstrated that dispersion contributions can be quite important to understanding substituent effects in $\pi-\pi$ interactions, especially for multiply substituted systems. In addition, SAPT analysis has uncovered the strong importance of charge-penetration terms in the physics of $\pi-\pi$ interactions. This is a critical finding because although $\pi-\pi$ interactions are ubiquitous in proteins and in DNA, these charge penetration terms are entirely absent in any popular force-field approach used in biomodeling. Hence, current force fields must rely on cancellations between the errors in the electrostatic terms and errors in other terms in order to achieve even semiquantitative accuracy for $\pi$-stacking interactions.[58] However, now that this deficiency is better understood, perhaps new efforts will be made to rectify it.

The recent availability of much faster SAPT algorithms[14−16,48] makes a much richer array of systems now accessible. Additionally, the easy availability of SAPT data could have a large impact on the development of next-generation force-field models. It is our belief that robust force-fields should be parametrized on a term-by-term basis (i.e., fitting electrostatic, London dispersion, exchange−repulsion, and induction terms separately), and high-quality SAPT data facilitates such an enterprise.

## BIOGRAPHICAL INFORMATION

**C. David Sherrill** was born in 1970. He received a Bachelor of Science degree from the Massachusetts Institute of Technology in 1992. He earned a Ph.D. in 1996 from the University of Georgia, working in the group of Professor Fritz Schaefer, and he was an NSF Postdoctoral Fellow in the group of Martin Head-Gordon at the University of California, Berkeley. Since 1999, he has been on the faculty at the Georgia Institute of Technology. He is a Fellow of the American Physical Society and the American Chemical Society.

## FOOTNOTES

## REFERENCES

1  Salonen, L. M.; Ellermann, M.; Diederich, F. Aromatic rings in chemical and biological recognition: Energetics and structures. *Angew. Chem., Int. Ed.* **2011**, *50*, 4808–4842.

2  Singh, N. J.; Min, S. K.; Kim, D. Y.; Kim, K. S. Comprehensive energy analysis for various types of π-interaction. *J. Chem. Theory Comput.* **2009**, *5*, 515–529.

3  Mati, I. K.; Cockroft, S. L. Molecular balances for quantifying non-covalent interactions. *Chem. Soc. Rev.* **2010**, *39*, 4195–4205.

4  Paliwal, S.; Geib, S.; Wilcox, C. S. Molecular torsion balance for weak molecular recognition forces. Effects of "tilted-T" edge-to-face aromatic interactions on conformational selection and solid-state structure. *J. Am. Chem. Soc.* **1994**, *116*, 4497–4498.

5  Kim, E.; Paliwal, S.; Wilcox, C. S. Measurements of molecular electrostatic field effects in edge-to-face aromatic interactions and CH−π interactions with implications for protein folding and molecular recognition. *J. Am. Chem. Soc.* **1998**, *120*, 11192–11193.

6  Nakamura, K.; Houk, K. N. Theoretical studies of the Wilcox molecular torsion balance. Is the edge-to-face aromatic interaction important? *Org. Lett.* **1999**, *1*, 2049–2051.

7  Ribas, J.; Cubero, E.; Luque, F. J.; Orozco, M. Theoretical study of alkyl-π and aryl-π interactions. reconciling theory and experiment. *J. Org. Chem.* **2002**, *67*, 7057–7065.

8  Sun, S.; Bernstein, E. R. Aromatic van der Waals clusters: Structure and nonrigidity. *J. Phys. Chem.* **1996**, *100*, 13348–13366.

9  Marshall, M. S.; Burns, L. A.; Sherrill, C. D. Basis set convergence of the coupled-cluster correction, $\delta_{MP2}^{CCSD(T)}$: Best practices for benchmarking non-covalent interactions and the attendant revision of the S22, NBC10, HBC6, and HSG databases. *J. Chem. Phys.* **2011**, *135*, No. 194102.

10  Jeziorski, B.; Moszynski, R.; Szalewicz, K. Perturbation theory approach to intermolecular potential energy surfaces of van der Waals complexes. *Chem. Rev.* **1994**, *94*, 1887–1930.

11  Szalewicz, K. Symmetry-adapted perturbation theory of intermolecular forces. *Wiley Interdiscip. Rev.: Comput. Mol. Sci.* **2012**, *2*, 254–272.

12  Lao, K. U.; Herbert, J. M. Breakdown of the single-exchange approximation in third-order symmetry-adapted perturbation theory. *J. Phys. Chem. A* **2012**, *116*, 3042–3047.

13  Hohenstein, E. G.; Jaeger, H. M.; Carrell, E. J.; Tschumper, G. S.; Sherrill, C. D. Accurate interaction energies for problematic dispersion-bound complexes: Homogeneous dimers of NCCN, P₂, and PCCP. *J. Chem. Theory Comput.* **2011**, *7*, 2842–2851.

14  Hohenstein, E. G.; Sherrill, C. D. Density fitting and Cholesky decomposition approximations in symmetry-adapted perturbation theory: Implementation and application to probe the nature of π-π interactions in linear acenes. *J. Chem. Phys.* **2010**, *132* No. 184111.

15  Heßelmann, A.; Jansen, G.; Schütz, M. Density-functional theory-symmetry-adapted intermolecular perturbation theory with density fitting: A new efficient method to study intermolecular interaction energies. *J. Chem. Phys.* **2005**, *122*, No. 014103.

16  Bukowski, R.; Podeszwa, R.; Szalewicz, K. Efficient calculation of coupled Kohn-Sham dynamic susceptibility functions and dispersion energies with density fitting. *Chem. Phys. Lett.* **2005**, *414*, 111–116.

17  Podeszwa, R.; Rice, B. M.; Szalewicz, K. Predicting structure of molecular crystals from first principles. *Phys. Rev. Lett.* **2008**, *101*, No. 115503.

18  Dougherty, D. A. Cation-π interactions in chemistry and biology: A new view of benzene, Phe, Tyr, and Trp. *Science* **1996**, *271*, 163–168.

19  Sunner, J.; Nishizawa, K.; Kerbarle, P. Ion-solvent molecule interactions in the gas-phase: The potassium-ion and benzene. *J. Phys. Chem.* **1981**, *85*, 1814.

20  Hohenstein, E. G.; Sherrill, C. D. Wavefunction methods for noncovalent interactions. *Wiley Interdiscip. Rev.: Comput. Mol. Sci.* **2012**, *2*, 304–326.

21  Marshall, M. S.; Steele, R. P.; Thanthiriwatte, K. S.; Sherrill, C. D. Potential energy curves for cation−π interactions: Off-axis configurations are also attractive. *J. Phys. Chem. A.* **2009**, *113*, 13628–13632.

22  Tsuzuki, S.; Yoshida, M.; Uchimaru, T.; Mikami, M. The origin of the cation/pi interaction: The significant importance of the induction in Li⁺ and Na⁺ complexes. *J. Phys. Chem. A.* **2001**, *105*, 769–773.

23  Meyer, E. A.; Castellano, R. K.; Diederich, F. Interactions with aromatic rings in chemical and biological recognition. *Angew. Chem., Int. Ed.* **2003**, *42*, 1210–1250.

24 Černý, J.; Kabeláč, M.; Hobza, P. Double-helical → ladder structural transition in the B-DNA is induced by a loss of dispersion energy. *J. Am. Chem. Soc.* **2008**, *130*, 16055–16059.

25 Cozzi, F.; Cinquini, M.; Annuziata, R.; Dwyer, T.; Siegel, J. S. Polar/$\pi$ interactions between stacked aryls in 1,8-diarylnaphthalenes. *J. Am. Chem. Soc.* **1992**, *114*, 5729–5733.

26 Mei, X.; Wolf, C. Highly congested nondistorted diheteroarylnaphthalenes: Model compounds for the investigation of intramolecular pi-stacking interactions. *J. Org. Chem.* **2005**, *70*, 2299–2305.

27 Wheeler, S. E.; McNeil, A. J.; Mueller, P.; Swager, T. M.; Houk, K. N. Probing substituent effects in aryl-aryl interactions using stereoselective diels alder cycloadditions. *J. Am. Chem. Soc.* **2010**, *132*, 3304–3311.

28 Chong, Y. S.; Carroll, W. R.; Burns, W. G.; Smith, M. D.; Shimizu, K. D. A high-barrier molecular balance for studying face-to-face arene-arene interactions in the solid state and in solution. *Chem.—Eur. J.* **2009**, *15*, 9117–9126.

29 Tsuzuki, S.; Honda, K.; Uchimaru, T.; Mikami, M.; Tanabe, K. Origin of attraction and directionality of the $\pi$-$\pi$ interaction: Model chemistry calculations of benzene dimer interaction. *J. Am. Chem. Soc.* **2002**, *124*, 104–112.

30 Sinnokrot, M. O.; Valeev, E. F.; Sherrill, C. D. Estimates of the ab initio limit for $\pi$-$\pi$ interactions: The benzene dimer. *J. Am. Chem. Soc.* **2002**, *124*, 10887–10893.

31 Hunter, C. A.; Sanders, J. K. M. The nature of $\pi$-$\pi$ Interactions. *J. Am. Chem. Soc.* **1990**, *112*, 5525–5534.

32 Sinnokrot, M. O.; Sherrill, C. D. Unexpected substituent effects in face-to-face $\pi$-stacking interactions. *J. Phys. Chem. A* **2003**, *107*, 8377–8379.

33 Sinnokrot, M. O.; Sherrill, C. D. Highly accurate coupled cluster potential energy curves for benzene dimer: The sandwich, T-shaped, and parallel-displaced configurations. *J. Phys. Chem. A* **2004**, *108*, 10200–10207.

34 Sinnokrot, M. O.; Sherrill, C. D. Substituent effects in $\pi$-$\pi$ interactions: Sandwich and T-shaped configurations. *J. Am. Chem. Soc.* **2004**, *126*, 7690–7697.

35 Wheeler, S. E.; Houk, K. N. Substituent effects in the benzene dimer are due to direct interactions of the substituents with the unsubstituted benzene. *J. Am. Chem. Soc.* **2008**, *130*, 10854–10855.

36 Rashkin, M. J.; Waters, M. L. Unexpected substituent effects in offset $\pi$-$\pi$ stacked interactions in water. *J. Am. Chem. Soc.* **2002**, *124*, 1860–1861.

37 Cockroft, S. L.; Perkins, J.; Zonta, C.; Adams, H.; Spey, S. E.; Low, C. M. R.; Vinter, J. G.; Lawson, K. R.; Urch, C. J.; Hunter, C. A. Substituent effects on aromatic stacking interactions. *Org. Biomol. Chem.* **2007**, *5*, 1062–1080.

38 Ringer, A. L.; Sinnokrot, M. O.; Lively, R. P.; Sherrill, C. D. The effect of multiple substituents on sandwich and T-shaped $\pi$-$\pi$ interactions. *Chem.—Eur. J.* **2006**, *12*, 3821–3828.

39 Wheeler, S. E.; Houk, K. N. Origin of substituent effects in edge-to-face aryl-aryl interactions. *Mol. Phys.* **2009**, *107*, 749–760.

40 Wheeler, S. E.; Houk, K. N. Through-space effects of substituents dominate molecular electrostatic potentials of substituted arenes. *J. Chem. Theory Comput.* **2009**, *5*, 2301–2312.

41 Wheeler, S. E.; Houk, K. N. Substituent effects in cation/$\pi$ interactions and electrostatic potentials above the centers of substituted benzenes are due primarily to through-space effects of the substituents. *J. Am. Chem. Soc.* **2009**, *131*, 3126–3127.

42 Wheeler, S. E. Local nature of substituent effects in stacking interactions. *J. Am. Chem. Soc.* **2011**, *133*, 10262–10274.

43 Ringer, A. L.; Sherrill, C. D. Substituent effects in sandwich configurations of multiply substituted benzene dimers are not solely governed by electrostatic control. *J. Am. Chem. Soc.* **2009**, *131*, 4574–4575.

44 Xia, J. L.; Liu, S. H.; Cozzi, F.; Mancinelli, M.; Mazzanti, A. An experimental study on the effect of substituents on aromatic-aromatic interactions in dithia[3,3]-metaparacyclophanes. *Chem.—Eur. J.* **2012**, *18*, 3611–3620.

45 Cockroft, S. L.; Hunter, C. A. Desolvation tips the balance: Solvent effects on aromatic interactions. *Chem. Commun.* **2006**, *45*, 3806–3808.

46 Cockroft, S. L.; Hunter, C. A. Desolvation and substituent effects in edge-to-face aromatic interactions. *Chem. Commun.* **2009**, *4*, 3961–3963.

47 Lee, E. C.; Hong, B. H.; Lee, J. Y.; Kim, J. C.; Kim, D.; Kim, Y.; Tarakeshwar, P.; Kim, K. S. Substituent effects on edge-to-face aromatic interactions. *J. Am. Chem. Soc.* **2005**, *127*, 4530–4537.

48 Hohenstein, E. G.; Parrish, R. M.; Sherrill, C. D.; Turney, J. M.; Schaefer, H. F. Large-scale symmetry-adapted perturbation theory computations via density fitting and Laplace transformation techniques: Investigating the fundamental forces of DNA-intercalator interactions. *J. Chem. Phys.* **2011**, *135*, No. 174107.

49 Watt, M.; Hardebeck, L. K. E.; Kirkpatrick, C. C.; Lewis, M. Face-to-face arene-arene binding energies: Dominated by dispersion but predicted by electrostatic and dispersion/polarizability substituent constants. *J. Am. Chem. Soc.* **2011**, *133*, 3854–3862.

50 Hohenstein, E. G.; Duan, J.; Sherrill, C. D. Origin of the surprising enhancement of electrostatic energies by electron-donating substituents in substituted sandwich benzene dimers. *J. Am. Chem. Soc.* **2011**, *133*, 13244–13247.

51 Lee, E. C.; Kim, D.; Jurečka, P.; Tarakeshwar, P.; Hobza, P.; Kim, K. S. Understanding of assembly phenomena by aromatic-aromatic interactions: Benzene dimer and the substituted systems. *J. Phys. Chem. A* **2007**, *111*, 3446–3457.

52 Arnstein, S. A.; Sherrill, C. D. Substituent effects in parallel-displaced $\pi$-$\pi$ interactions. *Phys. Chem. Chem. Phys.* **2008**, *10*, 2646–2655.

53 Seo, J.; Kim, I.; Lee, Y. S. Pi-pi interaction energies in monosubstituted-benzene dimers in parallel- and antiparallel-displaced conformations. *Chem. Phys. Lett.* **2009**, *474*, 101–106.

54 Hohenstein, E. G.; Sherrill, C. D. Effects of heteroatoms on aromatic $\pi$-$\pi$ interactions: Benzene-pyridine and pyridine dimer. *J. Phys. Chem. A* **2009**, *113*, 878–886.

55 Bates, D. M.; Anderson, J. A.; Oloyede, P.; Tschumper, G. S. Probing the effects of heterogeneity on delocalized $\pi$-$\pi$ interaction energies. *Phys. Chem. Chem. Phys.* **2008**, *10*, 2775–2779.

56 Geronimo, I.; Lee, E. C.; Singh, N. J.; Kim, K. S. How different are electron-rich and electron-deficient pi interactions? *J. Chem. Theory Comput.* **2010**, *6*, 1931–1934.

57 Maehigashi, T.; Persil, O.; Hud, N. V.; Williams, L. D. Unpublished results. Nucleic acid database (NDB) ID DD0103.

58 Sherrill, C. D.; Sumpter, B. G.; Sinnokrot, M. O.; Marshall, M. S.; Hohenstein, E. G.; Walker, R. C.; Gould, I. R. Assessment of standard force field models against high-quality ab initio potential curves for prototypes of $\pi$-$\pi$, CH/$\pi$, and SH/$\pi$ interactions. *J. Comput. Chem.* **2009**, *30*, 2187–2193.